1 **Exclusively heteronuclear NMR experiments for the investigation of intrinsically disordered**

2 **proteins: focusing on proline residues**

4 Isabella C. Felli[1], Wolfgang Bermel[2] and Roberta Pierattelli[1]

6 [1]CERM Department of Chemistry ''Ugo Schiff'', University of Florence, Via Luigi Sacconi 6, 50019 Sesto
7 Fiorentino, Florence, Italy
8 [2]Bruker BioSpin GmbH, Silberstreifen, 76287 Rheinstetten, Germany

10 *Corresponce to:*

11 Isabella C. Felli (felli@cerm.unifi.it) and Roberta Pierattelli (roberta.pierattelli@unifi.it)

13 **Keywords**

14 ^{13}C detection, IDP, NMR

16 **Abstract**

17 NMR represents a key spectroscopic technique to contribute to the emerging field of highly flexible,

18 intrinsically disordered proteins (IDPs) or protein regions (IDRs) that lack a stable three-dimensional

19 structure. A set of exclusively heteronuclear NMR experiments tailored for proline residues, highly

20 abundant in IDPs/IDRs, are presented here. They provide a valuable complement to the widely used

21 approach based on amide proton detection, filling the gap introduced by the lack of amide protons in

22 proline residues within polypeptide chains. The novel experiments have very interesting properties for

23 the investigations of IDPs/IDRs of increasing complexity.

24

25

Introduction

Invisible in X-ray studies of protein crystals, intrinsically disordered regions (IDRs) of complex proteins have been for a long time considered just passive linkers connecting functional globular domains and thus often ignored in structural biology studies. However, in many cases they comprise a significant fraction of the primary sequence of a protein and for this reason they are expected to have a role in protein function (Van Der Lee et al., 2014). The characterization of highly flexible regions of large proteins as well as entire proteins characterized by the lack of a 3D structure, now generally referred to as intrinsically disordered proteins (IDPs), lies well behind that of their folded counterparts and is nowadays pursued by an increasingly large number of studies to fill this knowledge gap. NMR plays a strategic role in this context since it constitutes the major, if not the unique, spectroscopic technique to achieve atomic resolution information on their structural and dynamic properties. However, intrinsic disorder and high flexibility have very relevant effects for NMR investigations such as reduction of chemical shift dispersion as well as efficient exchange processes with the solvent due to the open conformations that, when approaching physiological pH and temperature, broaden amide proton resonances beyond detection. While several elegant experiments were proposed to exploit exchange processes with the solvent (Kurzbach et al., 2017; Olsen et al., 2020; Szekely et al., 2018; Thakur et al., 2013), in general initial NMR investigations of IDPs/IDRs are carried out in conditions in which these critical points are mitigated. Exchange broadening strongly depends on pH and temperature; conditions can be optimized to recover most of the amide proton resonances enabling the acquisition of amide proton detected triple resonance experiments needed for sequence-specific assignment of the resonances. However, in particular for proteins that are largely exposed to the solvent it may be interesting to study them near physiological pH and temperature conditions (Gil et al., 2013). In this context, ^{13}C direct detection NMR developed into a valuable alternative.

Although the intrinsic sensitivity of ^{13}C is lower with respect to that of ^{1}H, ^{13}C nuclear spins are characterized by a large chemical shift dispersion (Dyson, H. Jane; Wright, 2001) and, when coupled to ^{15}N nuclei, provide a well-defined fingerprint of a polypeptide (Bermel et al., 2006a; Hsu et al., 2009; Lopez et al., 2016; Schiavina et al., 2019). These features were exploited to design a suite of 3D experiments based on carbonyl-carbon direct detection for sequential assignment and to measure NMR observables (Felli and Pierattelli, 2014). These experiments, starting from ^{1}H polarization, exploit only heteronuclear chemical shifts in the indirect dimensions to maximize chemical shift dispersion (exclusively heteronuclear experiments) and can be used to study IDPs/IDRs also in conditions in which amide proton resonances are too broad to be detected. In addition, they reveal information about proline residues that lack the amide

57 proton when part of polypeptide chains and cannot be detected in 2D HN correlation experiments even

58 if pH and temperature conditions are optimized to reduce exchange broadening.

59 Proline residues are abundant in IDPs/IDRs and often occur in proline-rich sequences with repetitive units

60 (Theillet et al., 2014). Initial bioinformatics studies on the relative abundance of each amino acid in regions

61 of the protein that could not be observed in X-ray diffraction studies led to the classification of prolines

62 as "disorder promoting" amino acids (Dunker et al., 2008). Nevertheless proline, the only imino acid,

63 features a closed ring in its side chain which confers local rigidity compared to all other amino acids

64 (Williamson, 1994), as also exploited in FRET studies in which proline residues are used as rigid spacers to

65 measure distances (Schuler et al., 2005). These observations clearly show the importance of experimental

66 atomic resolution information on the structural and dynamic properties of proline residues to understand

67 their role in modulating protein function. While abundant information about proline residues in globular

68 protein folds is available either through NMR or X-ray studies (MacArthur and Thornton, 1991), including

69 several examples of cis-trans isomerization of peptide bonds involving proline nitrogen as molecular

70 switches (Lu et al., 2007), their characterization in highly flexible and disordered polypeptides is available

71 only in a handful of cases (Chaves-Arquero et al., 2018; Gibbs et al., 2017; Haba et al., 2013; Hošek et al.,

72 2016; Knoblich et al., 2009; Pérez et al., 2009; Piai et al., 2016)(Chhabra et al., 2018)(Ahuja et al., 2016)

73 and actually early studies on IDPs/IDRs routinely reported assignment statistics only considering all other

74 amino acids ("excluding prolines").

75 Here we would like to propose an experimental variant of the most widely used ^{13}C detected 3D

76 experiments for sequence-specific assignment of IDPs/IDRs to selectively pick up correlations involving

77 proline nitrogen nuclei and provide key complementary information to that obtained through amide

78 proton detected experiments. They can be collected in a shorter time with respect to standard 3D

79 experiments and provide a valuable addition to the current experimental protocols for the study of IDPs.

80

81 **Materials and methods**

82 Isotopically labelled α-synuclein (^{13}C and ^{15}N) was expressed and purified as previously described (Huang

83 et al., 2005). The NMR sample has 0.6 mM protein concentration in 20 mM phosphate buffer at pH 6.5

84 and 100 mM NaCl in H_2O with 5% D_2O for the lock signal.

85   Isotopically labelled CBP-ID4 (^{13}C and ^{15}N) was expressed and purified as previously described (Piai et al.,

86   2016). The NMR sample has 0.9 mM protein concentration in water buffer containing 20 mM TRIS, 50 mM

87   KCl, at pH 6.9, with 5% D_2O added for the lock signal.

88   NMR experiments were acquired at 288 K (for α-synuclein) and at 283K (for CBP-ID4) with a 16.4 T Bruker

89   AVANCE NEO spectrometer operating at 700.06 MHz ^{1}H, 176.05 MHz ^{13}C, and 70.97 MHz ^{15}N frequencies,

90   equipped with a 5 mm cryogenically cooled probehead optimized for ^{13}C direct detection (TXO). RF pulses

91   and carrier frequencies typically employed for the investigation of intrinsically disordered proteins were

92   used, except for the modifications introduced to zoom into the proline ^{15}N region. Carrier frequencies

93   were set to 4.7 ppm (^{1}H), 176.4 ([13]C'), 53.9 ([13]C$^\alpha$), 44.9 ([13]C^{ali}); the ^{15}N carrier was set to 137 ppm, in the

94   center of ^{15}N resonances of proline residues. Hard pulses were used for [1]H. Band selective ^{13}C pulses used

95   were Q5 and Q3 (Emsley and Bodenhausen, 1990) of 300 μs and 231 μs for 90° and 180° rotations

96   respectively; a 900 μs Q3 pulse centered at 53.9 ppm was used for selective inversion of C$^\alpha$. The ^{15}N pulse

97   to invert the ^{15}N proline resonances was a 8000 μs Reburp pulse (Geen and Freeman, 1991); all other [15]N

98   pulses were hard pulses. Decoupling was achieved with waltz65 (100 μs, 2.5 kHz) (Zhou et al., 2007) for

99   [1]H and with garp4 (250 μs, 1.0 kHz) (Shaka, A. J.; Barker, P. B.; Freeman, 1985) for [15]N. The MOCCA mixing

100   time (Felli et al., 2009; Furrer et al., 2004) in the (HCA)COCON^{Pro} experiment was 350 ms, constituted by

101   repeated $(\Delta\text{-}180°\text{-}\Delta)_{2n}$ units in which $\Delta=150$ μs and the 180° pulse was 91.6 μs).

102   The experimental parameters used for the acquisition of the various experiments on α-synuclein and CBP-

103   ID4 are reported in Table 1. Spectra were calibrated using DSS as a reference for ^{1}H and ^{13}C; ^{15}N was

104   calibrated indirectly (Markley et al., 1998).

105   **Table 1.** Experimental parameters used.

106

Experiments α-synuclein	Dimension of acquired data			Spectral width (ppm)			NS[a]	$d_1(s)$[b]
	t1	t2	t3	F1	F2	F3		
[1]H detected								
^{1}H- ^{15}N HSQC	800 (^{15}N)	2048 (^{1}H)		28.1	15.0		2	1.0
[13]C detected								
CON	512 (^{15}N)	1024 (^{13}C)		32.0	31.0		2	1.6
CON[Pro]	128 (^{15}N)	1024 (^{13}C)		5.0	31.0		2	1.6
(H)CBCACON[Pro]	128 (^{13}C)	32 (^{15}N)	1024 (^{13}C)	60.0	5.0	30.0	4	1.0
(H)CCCON[Pro]	128 (^{13}C)	32 (^{15}N)	1024 (^{13}C)	70.0	5.0	30.0	4	1.0
(H)CBCANCO[Pro]	128 (^{13}C)	16 (^{15}N)	1024 (^{13}C)	60.0	5.0	30.0	8	1.0
[1]H and ^{13}C detected (using multiple receivers)								
CON/HN	600 (^{15}N)	1024 (^{13}C)		35.0	31.0		2	1.6
	600 (^{15}N)	2048 (^{1}H)		35.0	15.0		4	

Experiments CBP-ID4	Dimension of acquired data			Spectral width (ppm)			NS[a]	$d_1(s)$[b]
	t1	t2	t3	F1	F2	F3		
[1]H detected								
^{1}H- ^{15}N HSQC	800 (^{15}N)	2048 (^{1}H)		30.0	15.0		2	1.0
[13]C detected								
CON	1024 (^{15}N)	1024 (^{13}C)		38.0	30.0		2	2.0
CON[Pro]	170 (^{15}N)	1024 (^{13}C)		6.5	30.0		2	2.0
(H)CBCACON[Pro]	128 (^{13}C)	64 (^{15}N)	1024 (^{13}C)	64.5	6.5	30.0	4	1.0
(H)CCCON[Pro]	128 (^{13}C)	64 (^{15}N)	1024 (^{13}C)	75.7	6.5	30.0	4	1.0
(H)CBCANCO[Pro]	128 (^{13}C)	22 (^{15}N)	1024 (^{13}C)	64.5	6.5	30.0	16	1.0
(HCA)COCON[Pro]	96 (^{13}C)	64 (^{15}N)	1024 (^{13}C)	10.8	6.5	30.0	8	1.5

[a] number of acquired scans	
[b] inter-scan delay	

107

108   **Results and discussion**

109   *Advantages of focusing on proline residues*

110   In highly flexible and disordered proteins contributions to signals' chemical shifts deriving from the local

111   environment are averaged out leaving mainly those contributions due to the covalent structure of the

112   polypeptide. Chemical shift ranges predicted for ^{15}N resonances of imino acids such as proline are quite

113   different from those predicted for amino acids, as expected from the different chemical structure. The 2D

114   CON spectra of several disordered proteins of different size and sequence complexity, reported in Figure

115   1, clearly show that proline residues are quite abundant in IDPs/IDRs and that indeed ^{15}N resonances of

116   proline residues fall in a well isolated spectral region.

117
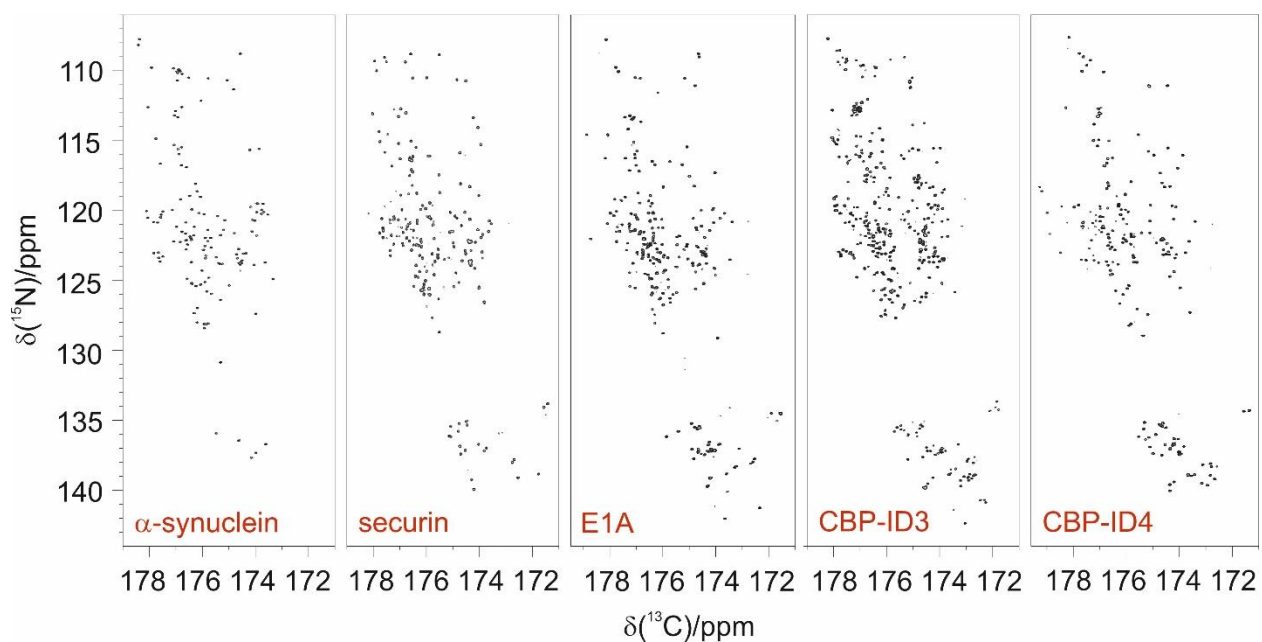
118

119   **Figure 1**. Proline residues are abundant in IDPs/IDRs and their ^{15}N resonances can be easily detected. They
120   fall in a specific, isolated region of the 2D CON spectrum as illustrated by the examples reported in the
121   figure. From left to right: α-synuclein (140 aa, 4% Pro)(Bermel et al., 2006b); human securin (200 aa, 11%
122   Pro)(Bermel et al., 2009); E1A (243 aa, 16% Pro)(Hošek et al., 2016); CBP-ID3 (407 aa 18% Pro)(Contreras-
123   Martos et al., 2017); CBP-ID4 (207 aa, 22% Pro)(Piai et al., 2016).

124

125   Thus, ^{15}N resonances of proline residues in IDPs/IDRs can be selectively irradiated enabling us to focus on

126   this spectral region. This can be achieved through the use of band-selective ^{15}N pulses as shown for the

127   simple case of the CON experiment (Murrali et al., 2018): the selective CON spectrum in the proline region

128   (CON[Pro], Figure 2) provides the complementary information that is missing in 2D HN correlation

129   experiments, even when pH and temperature are optimized to enhance the detectability of amide protons

130   (Figure 2).

131
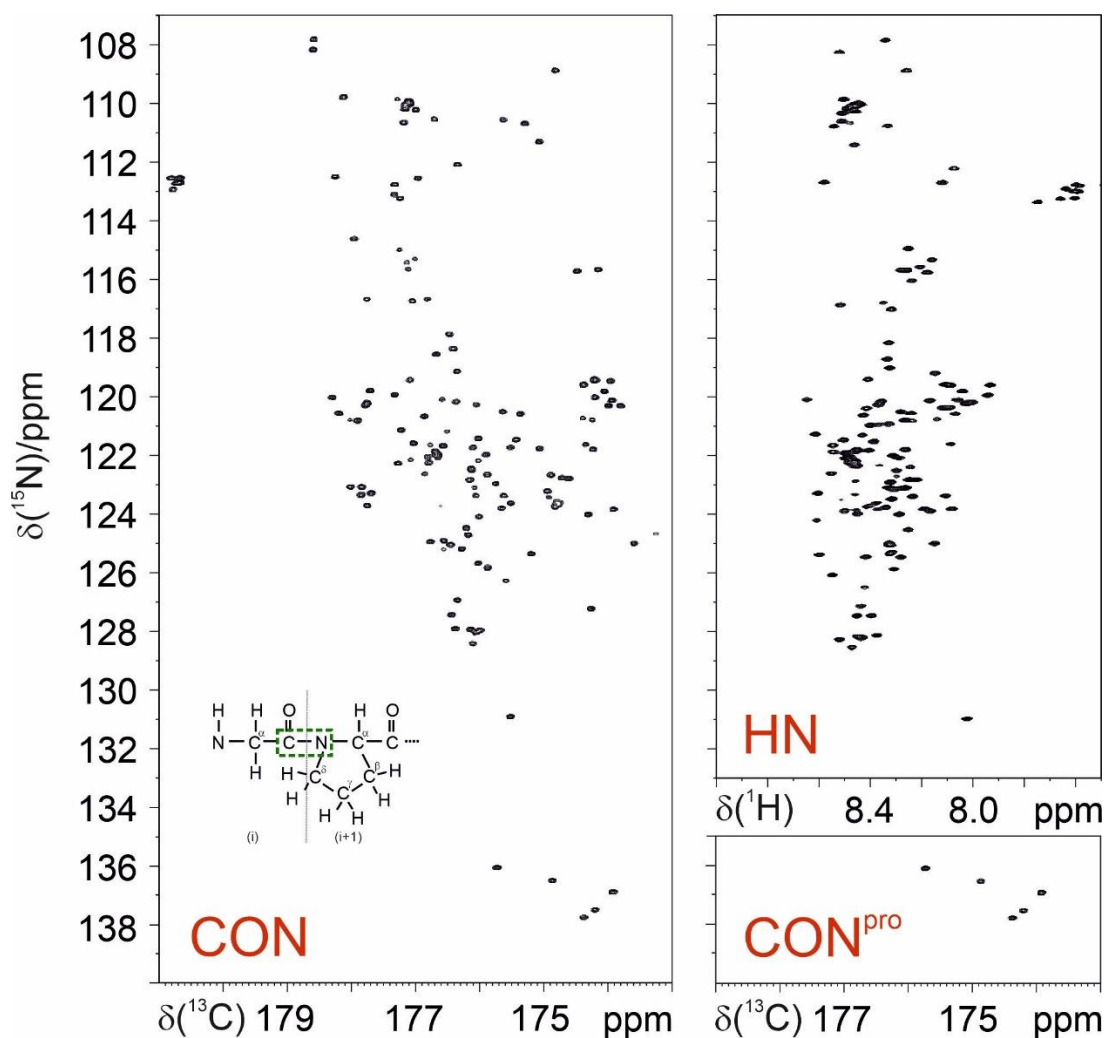
132

133

134   **Figure 2**. Comparison of the 2D CON (left) and 2D HN (right, top) spectra recorded on α-synuclein. The

135   CON[pro] spectrum (right, bottom), reported below the HN panel, clearly illustrates how this experiment

136   provides the missing information with respect to that available in the HN-detected spectrum. In the inset

137   of the 2D CON spectrum a scheme of a Gly_{i-1}-Pro_i dipeptide highlights the nuclei that give rise to the $C'_{i-1}N_i$

138   correlations detected in CON spectra (circled in green).

139 The same strategy exploiting band-selective ^{15}N pulses can be used to design experimental variants of

140 triple resonance ^{13}C detected experiments to focus on the ^{15}N proline region and enable us to selectively

141 detect the desired correlations. When implementing this idea into these experiments, such as the 3D

142 (H)CBCACON (Bermel et al., 2009), ^{15}N pulses could all be substituted with band-selective ones. However,

143 instead of substituting all ^{15}N pulses, it is sufficient to introduce a 180° band-selective ^{15}N pulse in one of

144 the C'_{i-1}-N_i coherence transfer steps to introduce the desired selectivity in the proline region.

145 As an example the pulse sequence of the 3D (H)CBCACON^{Pro} experiment is shown in Figure 3. The inclusion

146 of the ^{15}N band-selective pulse in the C'-N coherence transfer step is used to generate the C'_{i-1}-N_i antiphase

147 coherence ($2C'_yN_z$) involving the ^{15}N nuclear spin of proline residues (i); for all other amino acid types the

148 evolution of the C'_{i-1}-N_i scalar coupling ($^1J_{C'i-1Ni}$) is refocused by the 180° band-selective pulse on the

149 carbonyl carbon nuclei only. To achieve the desired selectivity on the ^{15}N proline resonances with respect

150 to those of all other amino acids an 8 ms Reburp pulse (Geen and Freeman, 1991) was used here; this

151 pulse may appear quite long, but it can be accommodated well in the C'-N coherence transfer block that

152 requires about 32 ms ($1/2^1J_{C'i-1Ni}$). Considering a 8-10 ppm spectral width necessary to cover the ^{15}N

153 proline-region in the indirect dimension (Figure 1), the implementation of this ^{15}N band-selective pulse

154 allows us to reduce the spectral width by a factor of about 4 with respect to that needed to cover the

155 whole spectral region in which backbone ^{15}N nuclear spins resonate, that is about 36-40 ppm. This means

156 that the same resolution can be achieved in a fraction of the time since ¼ (or less) of the FIDs should be

157 collected, provided sensitivity is not a limiting factor. Thus, it becomes feasible to acquire spectra with

158 very high resolution, extending the acquisition time in all the indirect dimensions to contrast the reduced

159 chemical shift dispersion typical of IDPs. Non-uniform sampling strategies (Hoch et al., 2014; Kazimierczuk

160 et al., 2010, 2011; Robson et al., 2019) can of course be implemented to reduce acquisition times; also in

161 this case reducing the spectral complexity (the number of cross-peaks is reduced when focusing on proline

162 ^{15}N resonances only) is expected to contribute to reducing experimental times. Out of the full 3D spectrum

163 only a small portion, the one containing the information that is completely missing in amide proton

164 detected experiments, can thus be acquired with the necessary resolution to provide site-specific atomic

165 information.

166 Since C' detected experiments all exploit the C'_{i-1}-N_i correlation, which is an inter-residue correlation

167 linking the nitrogen of an amino acid (i) to the carbonyl carbon of the previous one (i-1) across the peptide

168 bond (Figure 2 inset), focusing on proline residues can facilitate the identification of specific X_{i-1}-Pro_i pairs

169 through inspection of C^α and C^β chemical shifts of the amino acid preceding proline residues. Such

170   information can be achieved through the 3D (H)CBCACON^{Pro} experiment and can be very useful to identify

171   specific pairs such as Gly/Pro, Ala/Pro, Ser/Pro and Thr/Pro. Acquisition of the 3D (H)CCCON^{Pro}

172   experiment, in parallel to the 3D (H)CBCACON^{Pro}, provides information on aliphatic ^{13}C nuclear chemical

173   shifts of the whole side chain. This contributes to narrowing down the possibilities in all cases in which it

174   is not possible to identify the type of amino acid preceding the proline considering only their $^{13}C^{\alpha}$ and $^{13}C^{\beta}$

175   chemical shifts. This is the case for example of Arg/Lys/Gln or Phe/Leu.

176   Similarly, the insertion of the ^{15}N band-selective pulse in the proline region in the 3D (H)CBCANCO (Bermel

177   et al., 2006a) enables us to detect the ^{13}C resonances of the whole proline ring, providing the

178   complementary information for sequence-specific assignment. The closed proline ring introduces an

179   additional heteronuclear scalar coupling ($^{1}J_{Ni-C\delta i}$) that also provides the correlations with $^{13}C^{\delta}$ and $^{13}C^{\gamma}$, in

180   parallel to $^{13}C^{\alpha}$ and $^{13}C^{\beta}$ chemical shifts. Indeed the band-selective pulses used for the ^{13}C aliphatic region

181   cover also $^{13}C^{\gamma}$ and $^{13}C^{\delta}$ resonances (not only $^{13}C^{\alpha}$ and $^{13}C^{\beta}$ ones). In addition analysis of the observed

182   chemical shifts for proline side chains can be correlated to the local conformation, in particular to the

183   cis/trans isomers of the peptide bond involving proline nitrogen nuclei (Schubert et al., 2002; Shen and

184   Bax, 2010). Finally, additional information for sequence-specific assignment can be achieved by exploiting

185   the same approach for the COCON experiment in its ^{13}C-start (Bermel et al., 2006b; Felli et al., 2009) as

186   well and in its ^{1}H-start variants (Mateos et al., 2020).

187

188   *Assignment strategy*

189   To illustrate the approach, experiments were acquired on the well-known IDP α-synuclein. Even if this

190   protein only contains a little number of proline residues (5/140), they are all clustered in a small portion

191   of it (108-138) and thus constitute about 15% of the amino acids in this region. Furthermore, this terminus

192   has a very peculiar amino acidic composition (36% Asp/Glu, 9% Tyr) and it was shown to be the part of

193   the protein that is involved in sensing calcium concentration jumps associated with the transmission of

194   nerve signals (Binolfi et al., 2006; Lautenschläger et al., 2018; Nielsen et al., 2001). Proline residues,

195   embedded in two motifs (DPD and EPE), were shown to facilitate the interaction of carboxylate side chains

196   of Asp and Glu with calcium, even in a flexible and disordered state (Pontoriero et al., 2020).

197   Focusing on the proline ^{15}N region in case of α-synuclein greatly simplifies the spectral complexity enabling

198   us to illustrate the sequence-specific assignment of the resonances just by visual inspection of the first

199   planes of the 3D spectra described here (Figure 3).
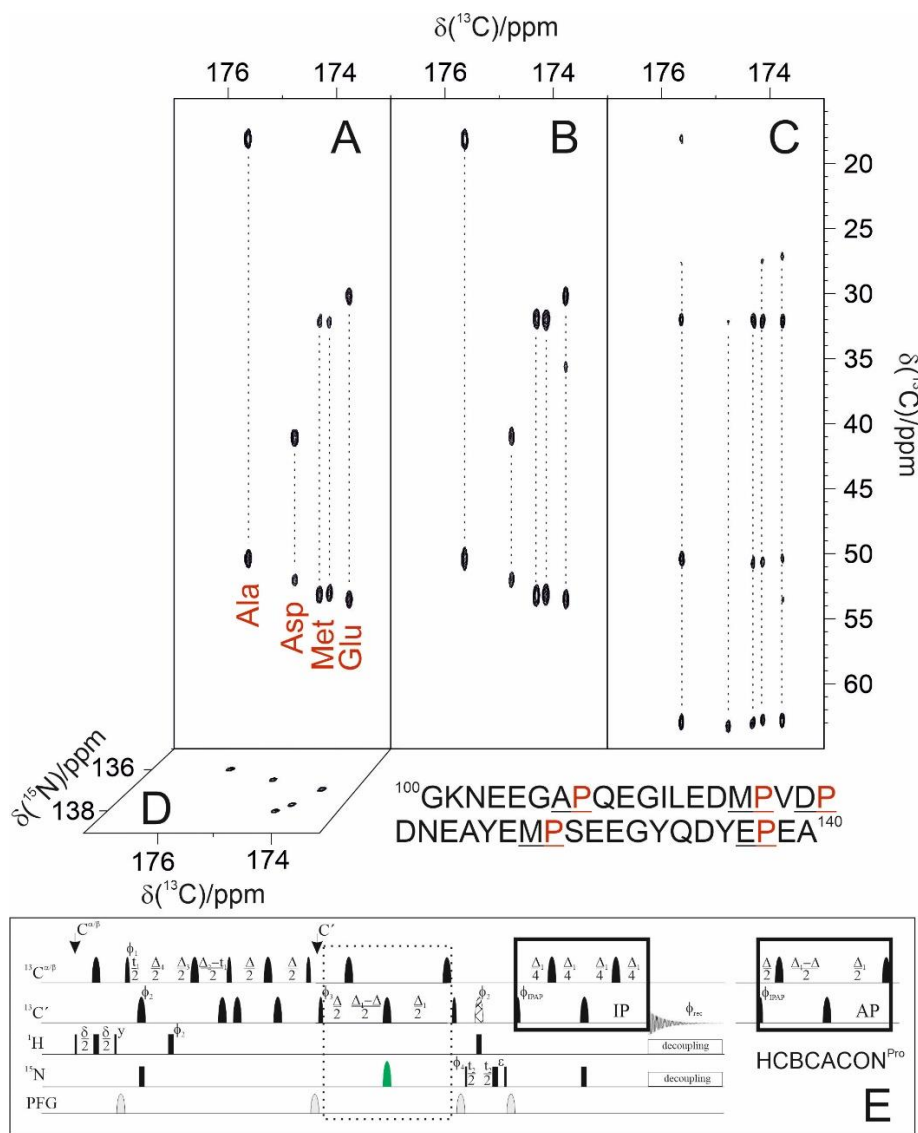
Figure 3. The implementation of the proposed strategy on α-synuclein renders NMR spectra so informative that proline resonances can be assigned just by visual inspection of the figure. To this end the first ^{13}C-^{13}C planes of the 3D (H)CBCACON^{Pro} (A), 3D (H)CCCON^{Pro} (B), 3D (H)CBCANCO^{Pro} (C) are shown; the ^{13}C-^{15}N plane of the 3D (H)CBCACON^{Pro} is also shown (D). The portion of the primary sequence of α-synuclein hosting its five proline residues is also reported (bottom right). The pulse sequence to acquire the 3D (H)CBCACON^{Pro} experiment (E) is reported as an example of the implementation of the proposed approach (dotted box). The delays are: ε = t$_2$(0), δ = 3.6 ms, Δ = 9 ms, Δ_1 = 25 ms, Δ_2 = 8 ms, Δ_3 = $\Delta_2-\Delta_4$ = 5.8 ms, Δ_4 = 2.2 ms. The phase cycle is: ϕ_1 = x, -x; ϕ_2 = 8(x), 8(-x); ϕ_3 = 4(x), 4(-x); ϕ_4 = 2(x), 2(-x); ϕ_{IPAP}(IP) = x; ϕ_{IPAP}(AP) = -y; ϕ_{rec} = x, -x, -x, x, -x, x, x, -x. Quadrature detection was obtained by incrementing phase ϕ_3 (t$_1$) and ϕ_4 (t$_2$) in a States-TPPI manner. The IPAP approach was implemented for homonuclear decoupling in the direct acquisition dimension to suppress the large one bond scalar coupling constants ($^1J_{C\alpha-C'}$)(Felli and Pierattelli, 2015); alternative approaches can be implemented that exploit band-selective homonuclear decoupling (Alik et al., 2020; Ying et al., 2014) or processing algorithms that thus only require the in-phase spectra (Karunanithy and Hansen, 2021; Shimba et al., 2003).

215   Indeed, the C'-N projections of the 3D spectra (^{13}C-^{15}N planes) show that the cross-peaks are well resolved

216   in both dimensions; selection of the ^{15}N proline region enables us to differentiate the signals through the

217   carbonyl carbon chemical shifts of the preceding amino acid. Therefore inspection of the first ^{13}C-^{13}C plane

218   of the 3D (H)CBCACON^{Pro} experiment (Figure 3A) shows the distinctive $^{13}C^{\alpha}$ and $^{13}C^{\beta}$ chemical shift patterns

219   of the residues preceding proline that, by comparison with the primary sequence of the protein, already

220   suggests us the identity of three residue pairs: Ala-Pro, Asp-Pro, Glu-Pro. These can thus be assigned to

221   Ala 107-Pro 108, Asp 119-Pro 120, Glu 138-Pro 139. Comparison with the first ^{13}C-^{13}C plane of the 3D

222   (H)CCCON^{Pro} (Figure 3B) confirms that an extra cross peak can be detected for the Glu-Pro pair, as

223   expected for amino acids which have a side chain with more than two aliphatic carbon atoms. The

224   remaining signals derive from the two Met-Pro pairs, in agreement with the observed chemical shifts.

225   They can be assigned in a sequence specific manner by comparison of these spectra with the

226   complementary ones based on amide proton detection. The final panel shows the first ^{13}C-^{13}C plane of

227   the 3D (H)CBCANCO^{Pro} (Figure 3C). This experiment reveals the correlations of the ^{15}N with $^{13}C^{\alpha}$ and $^{13}C^{\beta}$

228   within each amino acid. In the case of proline, the closed ring introduces additional scalar couplings that

229   are responsible for two additional cross-peaks, the ones of the ^{15}N with $^{13}C^{\gamma}$ and $^{13}C^{\delta}$, as clearly observed

230   in Figure 3. Chemical shifts show only minor differences between the resonances but still significant to

231   discriminate the different residues provided spectra are acquired with high resolution.

232

233   *A challenging case*

234   A compelling example of complexity is provided by the ID4 flexible linker of CREB-binding protein (CBP), a

235   large transcription co-regulator (Dyson and Wright, 2016). CBP-ID4 connects two well-characterized

236   globular domains (TAZ2, 92 amino acids and NCBD, 59 amino acids)(De Guzman et al., 2000; Kjaergaard

237   et al., 2010) and is constituted by 207 amino acids out of which 45 are proline residues, including several

238   repeated PP motifs (Piai et al., 2016) (Figure 4A). The 2D CON^{Pro} spectrum of CBP-ID4, reported in Figure

239   4B (left panel), shows the C'$_{i-1}$-N$_i$ correlations of proline residues of ID4. Interestingly, despite the small

240   spectral region, a high number of resolved resonances is observed. The initial count of cross-peaks in this

241   spectrum reveals 42 out of the 45 expected correlations, highlighting the potential of this experimental

242   strategy for the investigation of IDRs/IDPs of increasing complexity. The excellent chemical shift dispersion

243   of the inter-residue C'$_{i-1}$-N$_i$ correlations is certainly one of the most important aspects to reduce cross peak

244   overlap. Resolution is further enhanced in this region by the narrow linewidths of proline ^{15}N resonances

245   due to the lack of the dipolar contribution of an amide proton to the transverse relaxation.
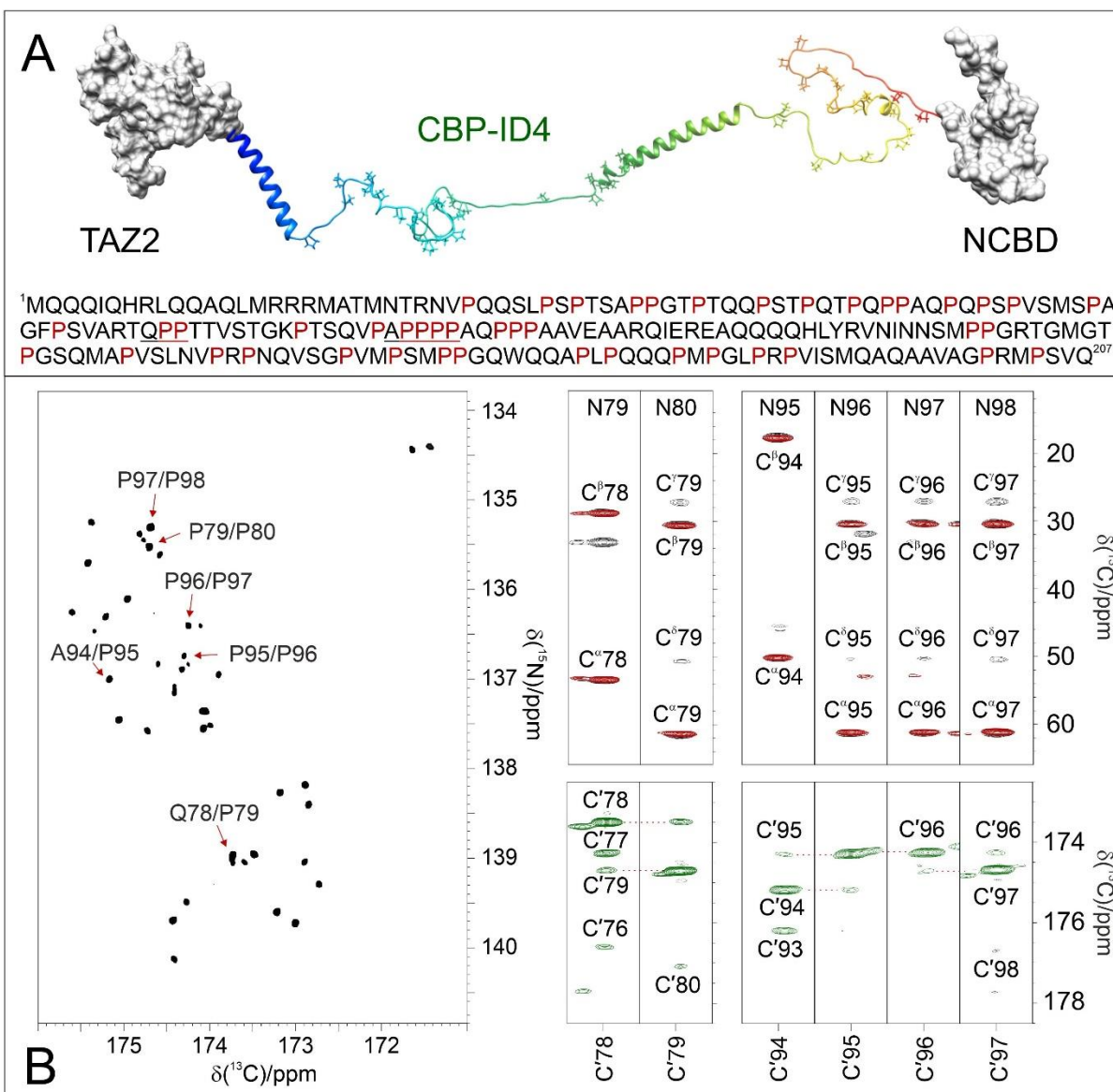
246

247

248 **Figure 4**. The case of CBP–ID4 (residues 1851–2057 of human CBP). (A) One of the possible conformations
249 of the CBP-ID4 fragment (blue-to-red ribbons) and the two flanking domains TAZ2 and NCBD clearly
250 demonstrate that in this region of CBP the intrinsically disordered part is highly prevalent with respect to
251 ordered ones. The amino acid sequence of CBP-ID4 is also reported. (B) The 2D CON[Pro] spectrum shown
252 on the left, which at first sight could seem like a 2D spectrum of a small globular protein, reports the
253 proline fingerprint of this complex IDR. Several strips extracted from the 3D (H)CBCACON[Pro] (black
254 contours), 3D (H)CCCON[Pro] (red contours), 3D (HCA)COCON[Pro] (green contours) are shown to illustrate the
255 information available for sequence specific resonance assignment of this proline-rich fragment of CBP-
256 ID4.

257   These two features contribute to establishing this spectral region as a key one for the assignment of a

258   large IDR. Indeed, when passing from 2D to 3D experiments, long acquisition times in the ^{15}N dimension

259   are possible and enable us to provide the extra contribution to resolution enhancement needed to focus

260   on complex IDRs and to collect additional information on the proline residues and their neighbouring

261   amino acids. As an example of the quality of the spectra, Figure 4B reports several strips extracted from

262   the pro-selective 3D experiments that were essential for the investigation of a particularly proline-rich

263   region of ID4, the one in between two partially populated α-helices (Piai et al., 2016). This is composed by

264   27 prolines (out of 76 amino acids) which constitute 35% of the amino acids in this region including several

265   proline-rich motifs (PXP, PXXP, PP as well as PPP and PPPP). Figure 4B shows the strips, extracted from

266   the 3D proline-selective experiments, that were used to assign resonances in the two proline-rich regions,

267   78-80 (QPP) and 94-98 (APPP). The strips extracted from the 3D (H)CBCACON^{Pro} and 3D (H)CCCON^{Pro}

268   (Figure 4B, right panels, black and red contours respectively) are very useful to identify the X_{i-1}-Pro$_i$ pairs

269   that match in this case with a Gln-Pro and an Ala-Pro pair as well as several Pro-Pro ones. The 3D

270   (H)CBCANCO^{Pro} completes the picture providing information about ^{13}C resonances of each proline ring (C^{α},

271   C^{β}, C^{γ}, C^{δ}, not shown for sake of clarity of the figure). However in regions with a high abundance of proline

272   residues additional information is needed for their sequence-specific assignment. To this end the 3D

273   (HCA)COCON^{Pro} (Figure 4B, right panels, green contours) is very useful, as demonstrated for these two

274   proline-rich fragments. This experiment, which includes an isotropic mixing element in the carbonyl region

275   (MOCCA in this case (Felli et al., 2009; Furrer et al., 2004)), enables us to detect correlations of a carbonyl

276   with the neighbouring ones through the small $^{3}J_{C'C'}$ scalar couplings. In case of proline residues the most

277   intense cross-peak is generally observed for the preceding amino acid (C'$_{i-2}$). However additional peaks

278   are detected also with neighbouring ones and support the sequence-specific assignment process.

279   It is interesting to note, once the sequence-specific assignment becomes available, that C'$_{i-1}$-N$_i$ correlations

280   fall in distinctive spectral regions of the CON^{Pro} 2D spectrum, as already pointed out for selected residue

281   pairs such as Gly-Pro, Ser-Pro, Thr-Pro, Val-Pro (Murrali et al., 2018). For example, inspection of Figure 1

282   allows us to identify Gly-Pro pairs in all the CON spectra of different proteins from their characteristic

283   chemical shifts (in the top-right portion of the proline region). An additional contribution towards smaller

284   ^{15}N chemical shifts can also be identified in cases in which more than one proline follows a specific amino

285   acid-type such as for Ala-Pro, Met-Pro and Gln-Pro cross peaks that are shifted to lower ^{15}N chemical shifts

286   when an additional proline follows in the primary sequence. These effects are likely to originate from a

287   combination of effects deriving from the covalent structure (primary sequence in this case) as well as from

288   local conformations. Needless to say that the experimental investigation of these aspects in more detail

289   constitutes an important point to describe the structural and dynamic properties at atomic resolution of

290   the proline-rich parts of highly flexible IDRs. The proposed experiments are thus expected to become of

291   general applicability for studies of IDPs/IDRs in solution.

292   The data generated on proline-rich sequences are of course very relevant to populate databases such as

293   the Biological Magnetic Resonance Data Bank (BMRB, https://bmrb.io/) with more information on proline

294   residues in highly flexible protein regions. This in turn will generate more accurate reference data in

295   chemical shift databases to determine local structural propensities through the comparison of

296   experimental shifts with reference ones (Camilloni et al., 2012; Tamiola et al., 2010) improving our

297   understanding of the importance of transient secondary structure elements in determining protein

298   function. On this respect, CBP itself provides another enlightening example with CBP-ID3 (residues 674-

299   1079 of CBP), which features a high number of proline residues (75 out of 406 residues) representing 18%

300   of its primary sequence. The distribution in this case is along the entire sequence but less frequent toward

301   the end, where a β-strand conformation propensity is sampled (Contreras-Martos et al., 2017). Also in

302   this case the distribution of proline residues is important in shaping the conformational space accessible

303   to the polypeptide, facilitating the interaction with protein's partners. Determination of additional

304   observables, such as the $^3J_{C'C'}$ through the 3D (HCA)COCON^{Pro} experiment or of different ones through

305   modified experimental variants of these experiments are expected to contribute to the characterization

306   of novel motifs in IDRs/IDPs.

307   The experimental strategy proposed here focuses on a remarkably small spectral region which however

308   turns out to be one of the most interesting ones, in particular in the perspective of studying IDPs/IDRs of

309   increasing complexity, somehow reminiscent of other strategies that have been proposed in which only

310   selected residue types are investigated to access information on challenging systems (such as for example

311   the studies of large systems enabled by Methyl-TROSY spectroscopy (Kay, 2011; Schütz and Sprangers,

312   2020). Interestingly the analysis of the NMR spectra presented here enables one to classify the observed

313   cross peaks into residue types, also in absence of sequence-specific assignment. This might provide

314   interesting information for complex IDPs/IDRs in which one is interested in the investigation of the

315   contribution of specific residue types, such as to monitor the occurrence of post-translational

316   modifications or even other phenomena that are more difficult to investigate like liquid-liquid phase

317   separation.

Conclusions and perspectives

Detection and assignment of proline-rich regions of highly flexible intrinsically disordered proteins allows us to have a glimpse on the ways in which proline residues encode specific properties in IDRs/IDPs by simply tuning their distribution along the primary sequence. NMR spectroscopy is particularly well suited for the task, since proline residues have attractive features from the NMR point of view, starting from the peculiar chemical shifts of ^{15}N nuclear spins. In addition, the lack of the attached amide proton implies that one of the major contributions to relaxation of ^{15}N spins is absent and thus proline nitrogen signals have small linewidths. These characteristics make them a very useful starting point for sequential assignment purposes and structure characterization. Furthermore, they provide a set of NMR signals with promising properties to enable high-resolution studies of increasingly large IDPs/IDRs.

Several approaches either based on H^N or on H$^\alpha$ direct detection have been proposed to bypass the problem introduced in sequence-specific assignment by the lack of amide protons typical of proline residues (Hellman et al., 2014; Kanelis et al., 2000; Karjalainen et al., 2020; Löhr et al., 2000; Mäntylahti et al., 2010; Tossavainen et al., 2020; Wong et al., 2018). While these can result useful for systems with moderate complexity (H$^\alpha$ detection) or for systems that feature isolated proline residues in the primary sequence (H^N/H$^\alpha$), they are not as efficient for complex IDRs/IDPs in which high resolution is mandatory and in which often consecutive proline residues are encountered. Detection of ^{15}N-based experiments can also provide direct observation of proline nuclei (Chhabra et al., 2018) but, despite the excellent resolution achievable with IDPs, these experiments still suffer from sensitivity limitations.

Concluding, the experiments proposed here are crucial to assign intrinsically disordered protein regions presenting many repeated motifs including proline residues as well as poly-proline segments reducing spectral complexity and experimental time without compromise in resolution. Since NMR probeheads with high ^{13}C sensitivity have become widely available, it is expected that this set of experiments will be applied as an easy-to-use tool also to complement H^N-based assignment.

Acknowledgments

The support of the CERM/CIRMMP center of Instruct-ERIC is gratefully acknowledged. This work has been funded in part by Fondazione CR Firenze and by the Italian Ministry of University and Research (FOE funding). Maria Grazia Murrali, Letizia Pontoriero and Marco Schiavina are acknowledged for their contribution in the early stages of the project.

References

Ahuja, P., Cantrelle, F. X., Huvent, I., Hanoulle, X., Lopez, J., Smet, C., Wieruszeski, J. M., Landrieu, I. and Lippens, G.: Proline conformation in a functional Tau fragment, J. Mol. Biol., 428(1), 79–91, doi:10.1016/j.jmb.2015.11.023, 2016.

Alik, A., Bouguechtouli, C., Julien, M., Bermel, W., Ghouil, R., Zinn-Justin, S. and Theillet, F. X.: Sensitivity-Enhanced ^{13}C-NMR spectroscopy for monitoring multisite phosphorylation at physiological temperature and pH, Angew. Chemie - Int. Ed., 1–6, doi:10.1002/anie.202002288, 2020.

Bermel, W., Bertini, I., Felli, I. C., Kümmerle, R. and Pierattelli, R.: Novel ^{13}C direct detection experiments, including extension to the third dimension, to perform the complete assignment of proteins, J. Magn. Reson., 178(1), 56–64, doi:10.1016/j.jmr.2005.08.011, 2006a.

Bermel, W., Bertini, I., Felli, I. C., Lee, Y.-M., Luchinat, C. and Pierattelli, R.: Protonless NMR experiments for sequence-specific assignment of backbone nuclei in unfolded proteins, J. Am. Chem. Soc., 128(12), 3918–3919, doi:10.1021/ja0582206, 2006b.

Bermel, W., Bertini, I., Csizmok, V., Felli, I. C., Pierattelli, R. and Tompa, P.: H-start for exclusively heteronuclear NMR spectroscopy: The case of intrinsically disordered proteins, J. Magn. Reson., 198(2), 275–281, doi:10.1016/j.jmr.2009.02.012, 2009.

Binolfi, A., Rasia, R. M., Bertoncini, C. W., Ceolin, M., Zweckstetter, M., Griesinger, C., Jovin, T. M. and Fernández, C. O.: Interaction of α-synuclein with divalent metal ions reveals key differences: A link between structure, binding specificity and fibrillation enhancement, J. Am. Chem. Soc., 128(30), 9893–9901, doi:10.1021/ja0618649, 2006.

Camilloni, C., De Simone, A., Vranken, W. F. and Vendruscolo, M.: Determination of secondary structure populations in disordered states of proteins using nuclear magnetic resonance chemical shifts, Biochemistry, 51(11), 2224–2231, doi:10.1021/bi3001825, 2012.

Chaves-Arquero, B., Pantoja-Uceda, D., Roque, A., Ponte, I., Suau, P. and Jiménez, M. A.: A CON-based NMR assignment strategy for pro-rich intrinsically disordered proteins with low signal dispersion: the C-terminal domain of histone H1.0 as a case study, J. Biomol. NMR, 72(3–4), 139–148, doi:10.1007/s10858-018-0213-2, 2018.

Chhabra, S., Fischer, P., Takeuchi, K., Dubey, A., Ziarek, J. J., Boeszoermenyi, A., Mathieu, D., Bermel, W., Davey, N. E., Wagner, G. and Arthanari, H.: ^{15}N detection harnesses the slow relaxation property of nitrogen: Delivering enhanced resolution for intrinsically disordered proteins, Proc. Natl. Acad. Sci., 115(8), E1710–E1719, doi:10.1073/pnas.1717560115, 2018.

Contreras-Martos, S., Piai, A., Kosol, S., Varadi, M., Bekesi, A., Lebrun, P., Volkov, A. N., Gevaert, K., Pierattelli, R., Felli, I. C. and Tompa, P.: Linking functions: An additional role for an intrinsically disordered linker domain in the transcriptional coactivator CBP, Sci. Rep., 7(1), 4676, doi:10.1038/s41598-017-04611-x, 2017.

Dunker, A. K., Oldfield, C. J., Meng, J., Romero, P., Yang, J. Y., Chen, J. W., Vacic, V., Obradovic, Z. and Uversky, V. N.: The unfoldomics decade: An update on intrinsically disordered proteins, BMC Genomics, 9(SUPPL. 2), 1–26, doi:10.1186/1471-2164-9-S2-S1, 2008.

Dyson, H. Jane; Wright, P.: Nuclear magnetic resonance methods for elucidation of structure and dynamics in disordered states, Methods Enzymol., 339, 258–270, 2001.

388 Dyson, H. J. and Wright, P. E.: Role of intrinsic protein disorder in the function and interactions of the
389 transcriptional coactivators CREB-binding Protein (CBP) and p300, J. Biol. Chem., 291(13), 6714–6722,
390 doi:10.1074/jbc.R115.692020, 2016.

391 Emsley, L. and Bodenhausen, G.: Gaussian pulse cascades: New analytical functions for rectangular
392 selective inversion and in-phase excitation in NMR, Chem. Phys. Lett., 165(6), 469–476,
393 doi:10.1016/0009-2614(90)87025-M, 1990.

394 Felli, I. C. and Pierattelli, R.: Novel methods based on ^{13}C detection to study intrinsically disordered
395 proteins, J. Magn. Reson., 241(1), 115–125, doi:10.1016/j.jmr.2013.10.020, 2014.

396 Felli, I. C. and Pierattelli, R.: Spin-state-selective methods in solution- and solid-state biomolecular [13]C
397 NMR, Prog. Nucl. Magn. Reson. Spectrosc., 84–85, 1–13, doi:10.1016/j.pnmrs.2014.10.001, 2015.

398 Felli, I. C., Pierattelli, R., Glaser, S. J. and Luy, B.: Relaxation-optimised Hartmann-Hahn transfer using a
399 specifically Tailored MOCCA-XY16 mixing sequence for carbonyl-carbonyl correlation spectroscopy in[13]C
400 direct detection NMR experiments, J. Biomol. NMR, 43(3), doi:10.1007/s10858-009-9302-6, 2009.

401 Furrer, J., Kramer, F., Marino, J. P., Glaser, S. J. and Luy, B.: Homonuclear Hartmann-Hahn transfer with
402 reduced relaxation losses by use of the MOCCA-XY16 multiple pulse sequence, J. Magn. Reson., 166(1),
403 39–46, doi:10.1016/j.jmr.2003.09.013, 2004.

404 Geen, H. and Freeman, R.: Band-selective radiofrequency pulses, J. Magn. Reson., 93(1), 93–141,
405 doi:10.1016/0022-2364(91)90034-Q, 1991.

406 Gibbs, E. B., Lu, F., Portz, B., Fisher, M. J., Medellin, B. P., Laremore, T. N., Zhang, Y. J., Gilmour, D. S. and
407 Showalter, S. A.: Phosphorylation induces sequence-specific conformational switches in the RNA
408 polymerase II C-terminal domain, Nat. Commun., 8(May), 1–11, doi:10.1038/ncomms15233, 2017.

409 Gil, S., Hošek, T., Solyom, Z., Kümmerle, R., Brutscher, B., Pierattelli, R. and Felli, I. C.: NMR spectroscopic
410 studies of intrinsically disordered proteins at near-physiological conditions, Angew. Chemie - Int. Ed.,
411 52(45), 11808–11812, doi:10.1002/anie.201304272, 2013.

412 De Guzman, R. N., Liu, H. Y., Martinez-Yamout, M., Dyson, H. J. and Wright, P. E.: Solution structure of
413 the TAZ2 (CH3) domain of the transcriptional adaptor protein CBP, J. Mol. Biol., 303(2), 243–253,
414 doi:10.1006/jmbi.2000.4141, 2000.

415 Haba, N. Y., Gross, R., Novacek, J., Shaked, H., Zidek, L., Barda-Saad, M. and Chill, J. H.: NMR determines
416 transient structure and dynamics in the disordered C-terminal domain of WASp interacting protein,
417 Biophys. J., 105(2), 481–493, doi:10.1016/j.bpj.2013.05.046, 2013.

418 Hellman, M., Piirainen, H., Jaakola, V. P. and Permi, P.: Bridge over troubled proline: Assignment of
419 intrinsically disordered proteins using (HCA)CON(CAN)H and (HCA)N(CA)CO(N)H experiments
420 concomitantly with HNCO and i(HCA)CO(CA)NH, J. Biomol. NMR, 58(1), 49–60, doi:10.1007/s10858-013-
421 9804-0, 2014.

422 Hoch, J. C., Maciejewski, M. W., Mobli, M., Schuyler, A. D. and Stern, A. S.: Nonuniform sampling and
423 maximum entropy reconstruction in multidimensional NMR, Acc. Chem. Res., 47(2), 708–717,
424 doi:10.1021/ar400244v, 2014.

425 Hošek, T., Calçada, E. O., Nogueira, M. O., Salvi, M., Pagani, T. D., Felli, I. C. and Pierattelli, R.: Structural
426 and dynamic characterization of the molecular hub early region 1A (E1A) from human adenovirus,
427 Chem. - A Eur. J., 22(37), doi:10.1002/chem.201602510, 2016.

Hsu, S.-T. D., Bertoncini, C. W. and Dobson, C. M.: Use of protonless NMR spectroscopy to alleviate the loss of information resulting from exchange-broadening, J. Am. Chem. Soc., 131(21), 7222–7223, doi:10.1021/ja902307q, 2009.

Huang, C., Ren, G., Zhou, H. and Wang, C.: A new method for purification of recombinant human α-synuclein in Escherichia coli, Protein Expr. Purif., 42(1), 173–177, doi:10.1016/j.pep.2005.02.014, 2005.

Kanelis, V., Donaldson, L., Muhandiram, D. R., Rotin, D., Forman-Kay, J. D. and Kay, L. E.: Sequential assignment of proline-rich regions in proteins: Application to modular binding domain complexes, J. Biomol. NMR, 16(3), 253–259, doi:10.1023/A:1008355012528, 2000.

Karjalainen, M., Tossavainen, H., Hellman, M. and Permi, P.: HACANCOi: a new Hα-detected experiment for backbone resonance assignment of intrinsically disordered proteins, J. Biomol. NMR, 74(12), 741–752, doi:10.1007/s10858-020-00347-5, 2020.

Karunanithy, G. and Hansen, D. F.: FID-Net: A versatile deep neural network architecture for NMR spectral reconstruction and virtual decoupling, J. Biomol. NMR, 75(4), 179–191, doi:10.1007/s10858-021-00366-w, 2021.

Kay, L. E.: Solution NMR spectroscopy of supra-molecular systems, why bother? A methyl-TROSY view, J. Magn. Reson., 210(2), 159–170, doi:10.1016/j.jmr.2011.03.008, 2011.

Kazimierczuk, K., Stanek, J., Zawadzka-Kazimierczuk, A. and Koźmiński, W.: Random sampling in multidimensional NMR spectroscopy, Prog. Nucl. Magn. Reson. Spectrosc., 57(4), 420–434, doi:10.1016/j.pnmrs.2010.07.002, 2010.

Kazimierczuk, K., Misiak, M., Stanek, J., Zawadzka-Kazimierczuk, A. and Koźmiński, W.: Generalized fourier transform for non-uniform sampled data, in Topics in current chemistry, vol. 312, pp. 79–124., 2011.

Kjaergaard, M., Teilum, K. and Poulsen, F. M.: Conformational selection in the molten globule state of the nuclear coactivator binding domain of CBP, Proc. Natl. Acad. Sci. U. S. A., 107(28), 12535–12540, doi:10.1073/pnas.1001693107, 2010.

Knoblich, K., Whittaker, S., Ludwig, C., Michiels, P., Jiang, T., Schaffhausen, B. and Günther, U.: Backbone assignment of the N-terminal polyomavirus large T antigen, Biomol. NMR Assign., 3(1), 119–123, doi:10.1007/s12104-009-9155-7, 2009.

Kurzbach, D., Canet, E., Flamm, A. G., Jhajharia, A., Weber, E. M. M., Konrat, R. and Bodenhausen, G.: Investigation of intrinsically disordered proteins through exchange with hyperpolarized water, Angew. Chemie - Int. Ed., 56(1), 389–392, doi:10.1002/anie.201608903, 2017.

Lautenschläger, J., Stephens, A. D., Fusco, G., Ströhl, F., Curry, N., Zacharopoulou, M., Michel, C. H., Laine, R., Nespovitaya, N., Fantham, M., Pinotsi, D., Zago, W., Fraser, P., Tandon, A., St George-Hyslop, P., Rees, E., Phillips, J. J., De Simone, A., Kaminski, C. F. and Schierle, G. S. K.: C-terminal calcium binding of α-synuclein modulates synaptic vesicle interaction, Nat. Commun., 9(1), doi:10.1038/s41467-018-03111-4, 2018.

Van Der Lee, R., Buljan, M., Lang, B., Weatheritt, R. J., Daughdrill, G. W., Dunker, A. K., Fuxreiter, M., Gough, J., Gsponer, J., Jones, D. T., Kim, P. M., Kriwacki, R. W., Oldfield, C. J., Pappu, R. V, Tompa, P., Uversky, V. N., Wright, P. E. and Babu, M. M.: Classification of intrinsically disordered regions and proteins, Chem. Rev., 114(13), 6589–6631, doi:10.1021/cr400525m, 2014.

Löhr, F., Pfeiffer, S., Lin, Y. J., Hartleib, J., Klimmek, O. and Rüterjans, H.: HNCAN pulse sequences for sequential backbone resonance assignment across proline residues in perdeuterated proteins, J. Biomol. NMR, 18(4), 337–346, doi:10.1023/A:1026737732576, 2000.

Lopez, J., Schneider, R., Cantrelle, F. X., Huvent, I. and Lippens, G.: Studying intrinsically disordered Proteins under true in vivo conditions by combined cross-polarization and carbonyl-detection NMR Spectroscopy, Angew. Chemie - Int. Ed., 55(26), 7418–7422, doi:10.1002/anie.201601850, 2016.

Lu, K. P., Finn, G., Lee, T. H. and Nicholson, L. K.: Prolyl cis-trans isomerization as a molecular timer, Nat. Chem. Biol., 3(10), 619–629, doi:10.1038/nchembio.2007.35, 2007.

MacArthur, M. W. and Thornton, J. M.: Influence of proline residues on protein conformation, J. Mol. Biol., 218(2), 397–412, doi:10.1016/0022-2836(91)90721-H, 1991.

Mäntylahti, S., Aitio, O., Hellman, M. and Permi, P.: HA-detected experiments for the backbone assignment of intrinsically disordered proteins, J. Biomol. NMR, 47(3), 171–181, doi:10.1007/s10858-010-9421-0, 2010.

Markley, J. L., Bax, A., Arata, Y., Hilbers, C. W., Kaptein, R., Sykes, B. D., Wright, P. E. and Wüthrich, K.: Recommendations for the presentation of NMR structures of proteins and nucleic acids, J. Biomol. NMR, 12(1), 1–23, doi:10.1023/A:1008290618449, 1998.

Mateos, B., Conrad-Billroth, C., Schiavina, M., Beier, A., Kontaxis, G., Konrat, R., Felli, I. C. and Pierattelli, R.: The ambivalent role of proline residues in an intrinsically disordered protein: From disorder promoters to compaction facilitators, J. Mol. Biol., 432(9), doi:10.1016/j.jmb.2019.11.015, 2020.

Murrali, M. G., Piai, A., Bermel, W., Felli, I. C. and Pierattelli, R.: Proline fingerprint in intrinsically disordered proteins, ChemBioChem, 19(15), 1625–1629, doi:10.1002/cbic.201800172, 2018.

Nielsen, M. S., Vorum, H., Lindersson, E. and Jensen, P. H.: Ca^{2+} Binding to α-synuclein regulates ligand binding and oligomerization, J. Biol. Chem., 276(25), 22680–22684, doi:10.1074/jbc.M101181200, 2001.

Olsen, G. L., Szekely, O., Mateos, B., Kadeřávek, P., Ferrage, F., Konrat, R., Pierattelli, R., Felli, I. C., Bodenhausen, G., Kurzbach, D. and Frydman, L.: Sensitivity-enhanced three-dimensional and carbon-detected two-dimensional NMR of proteins using hyperpolarized water, J. Biomol. NMR, 74(2–3), 161–171, doi:10.1007/s10858-020-00301-5, 2020.

Pérez, Y., Gairí, M., Pons, M. and Bernadó, P.: Structural characterization of the natively unfolded N-terminal domain of human c-Src kinase: insights into the role of phosphorylation of the unique domain., J. Mol. Biol., 391(1), 136–148, doi:10.1016/j.jmb.2009.06.018, 2009.

Piai, A., Calçada, E. O., Tarenzi, T., Grande, A. Del, Varadi, M., Tompa, P., Felli, I. C. and Pierattelli, R.: Just a flexible linker? the structural and dynamic properties of CBP-ID4 revealed by NMR spectroscopy, Biophys. J., 110(2), 372–381, doi:10.1016/j.bpj.2015.11.3516, 2016.

Pontoriero, L., Schiavina, M., Murrali, M. G., Pierattelli, R. and Felli, I. C.: Monitoring the Interaction of α-synuclein with calcium ions through exclusively heteronuclear Nuclear Magnetic Resonance experiments, Angew. Chemie, 132(42), 18696–18704, doi:10.1002/ange.202008079, 2020.

Robson, S., Arthanari, H., Hyberts, S. G. and Wagner, G.: Nonuniform sampling for NMR spectroscopy, in Methods Enzymol., pp. 263–291., 2019.

Schiavina, M., Murrali, M. G., Pontoriero, L., Sainati, V., Kümmerle, R., Bermel, W., Pierattelli, R. and

507   Felli, I. C.: Taking simultaneous snapshots of intrinsically disordered proteins in action, Biophys. J.,
508   117(1), doi:10.1016/j.bpj.2019.05.017, 2019.

509   Schubert, M., Labudde, D., Oschkinat, H. and Schmieder, P.: A software tool for the prediction of Xaa-Pro
510   peptide bond conformations in proteins based on 13C chemical shift statistics, J. Biomol. NMR, 24(2),
511   149–154, doi:10.1023/A:1020997118364, 2002.

512   Schuler, B., Lipman, E. A., Steinbach, P. J., Kumke, M. and Eaton, W. A.: Polyproline and the
513   "spectroscopic ruler" revisited with single-molecule fluorescence., Proc. Natl. Acad. Sci. U. S. A., 102(8),
514   2754–9, doi:10.1073/pnas.0408164102, 2005.

515   Schütz, S. and Sprangers, R.: Methyl TROSY spectroscopy: A versatile NMR approach to study challenging
516   biological systems, Prog. Nucl. Magn. Reson. Spectrosc., 116, 56–84, doi:10.1016/j.pnmrs.2019.09.004,
517   2020.

518   Shaka, A. J.; Barker, P. B.; Freeman, R.: Computer-optimized decoupling scheme for wideband
519   applications and low-level operation, J. Magn. Reson., 64(547), 552, 1985.

520   Shen, Y. and Bax, A.: Prediction of Xaa-Pro peptide bond conformation from sequence and chemical
521   shifts, J. Biomol. NMR, 46(3), 199–204, doi:10.1007/s10858-009-9395-y, 2010.

522   Shimba, N., Stern, A. S., Craik, C. S., Hoch, J. C. and Dötsch, V.: Elimination of ^{13}Cα splitting in protein
523   NMR spectra by deconvolution with maximum entropy reconstruction, J. Am. Chem. Soc., 125(9), 2382–
524   2383, doi:10.1021/ja027973e, 2003.

525   Szekely, O., Olsen, G. L., Felli, I. C. and Frydman, L.: High-resolution 2D NMR of disordered proteins
526   enhanced by hyperpolarized water, , doi:10.1021/acs.analchem.8b00585, 2018.

527   Tamiola, K., Acar, B. and Mulder, F. A. A.: Sequence-specific random coil chemical shifts of intrinsically
528   disordered proteins, J. Am. Chem. Soc., 132(51), 18000–18003, doi:10.1021/ja105656t, 2010.

529   Thakur, A., Chandra, K., Dubey, A., D'Silva, P. and Atreya, H. S.: Rapid characterization of hydrogen
530   exchange in proteins, Angew. Chemie - Int. Ed., 52(9), 2440–2443, doi:10.1002/anie.201206828, 2013.

531   Theillet, F., Kalmar, L., Tompa, P., Han, K., Selenko, P., Dunker, A. K., Daughdrill, G. W. and Uversky, V. N.:
532   The alphabet of intrinsic disorder, Intrinsically Disord. Proteins, 1(April), e24360, doi:10.4161/idp.24360,
533   2014.

534   Tossavainen, H., Salovaara, S., Hellman, M., Ihalin, R. and Permi, P.: Dispersion from Cα or NH: 4D
535   experiments for backbone resonance assignment of intrinsically disordered proteins, J. Biomol. NMR,
536   74(2–3), 147–159, doi:10.1007/s10858-020-00299-w, 2020.

537   Williamson, M. P.: The structure and function of proline-rich regions in proteins, Biochem. J., 297(2),
538   249–260, doi:10.1042/bj2970249, 1994.

539   Wong, L. E., Maier, J., Wienands, J., Becker, S. and Griesinger, C.: Sensitivity-enhanced four-dimensional
540   amide–amide correlation NMR experiments for sequential assignment of proline-rich disordered
541   proteins, J. Am. Chem. Soc., 140(10), 3518–3522, doi:10.1021/jacs.8b00215, 2018.

542   Ying, J., Li, F., Lee, J. H. and Bax, A.: ^{13}Cα decoupling during direct observation of carbonyl resonances in
543   solution NMR of isotopically enriched proteins, J. Biomol. NMR, 60(1), 15–21, doi:10.1007/s10858-014-
544   9853-z, 2014.

545   Zhou, Z., Kümmerle, R., Qiu, X., Redwine, D., Cong, R., Taha, A., Baugh, D. and Winniford, B.: A new

546   decoupling method for accurate quantification of polyethylene copolymer composition and triad
547   sequence distribution with ^{13}C NMR, J. Magn. Reson., 187(2), 225–233, doi:10.1016/j.jmr.2007.05.005,
548   2007.

549